Neuron, Vol. 42, 63–75, April 8, 2004, Copyright ©2004 by Cell Press

Diverse Functions of N-Cadherin in Dendritic and Axonal Terminal Arborization of Olfactory Projection Neurons

Haitao Zhu and Liqun Luo*
Department of Biological Sciences
Stanford University
Stanford, California 94305

Summary

The cadherin superfamily of cell adhesion molecules have been proposed to play important roles in determining synaptic specificity in developing nervous systems. We examine the function of N-cadherin in *Drosophila* second order olfactory projection neurons (PNs), each of which must selectively target their dendrites to one of ~50 glomeruli. Our results do not support an instructive role for N-cadherin in selecting dendritic targets; rather, N-cadherin is essential for PNs to restrict their dendrites to single glomeruli. Mosaic analyses suggest that N-cadherin mediates dendro-dendritic interactions between PNs and thus contributes to refinement of PN dendrites to single glomeruli. N-cadherin is also essential for the development of PN axon terminal arbors in two distinct central targets: regulating branch stability in the lateral horn and restricting high-order branching in the mushroom body. Although the *N-cadherin* locus potentially encodes eight alternatively spliced isoforms, transgenic expression of one isoform is sufficient to rescue all phenotypes.

Introduction

The olfactory neural circuit presents a fascinating wiring problem. From flies to mammals, olfactory receptor neurons (ORNs) expressing a common olfactory receptor have widely distributed cell body positions in sensory epithelia, yet their axons converge onto the same glomeruli in the antennal lobe/olfactory bulb, thereby forming the first spatial odor map in the brain (reviewed in Axel, 1995; Buck, 2000; Keller and Vosshall, 2003). In *Drosophila*, second order olfactory projection neurons (PNs), the main postsynaptic targets of ORNs, send dendrites into specific glomeruli according to their lineage and birth order (Jefferis et al., 2001). Furthermore, PNs of a particular glomerular class exhibit stereotypical axon branching patterns and terminal fields in the lateral horn, one of the higher order olfactory centers, allowing stereotypical transfer and transformation of olfactory information farther into the brain (Marin et al., 2002; Wong et al., 2002). Thus, during the construction of the fly olfactory system, a given ORN must choose one of ~50 glomeruli to target its axons, while a given PN must also choose one of ~50 glomeruli to target its dendrites, and furthermore the PN must coordinate its dendritic target choice with its axon terminal arborization pattern in higher olfactory centers. Evidence suggests that at least the initial development of the olfactory circuit is independent of sensory input (Jefferis et al., 2002); for instance, the antennal lobe glomerular assembly, as well as the axon terminal arborization pattern, are largely complete before the first signs of olfactory receptor expression (Jefferis et al., 2004). Thus, wiring seems to be controlled predominantly by genetic programs. The molecular logic that underlies this striking wiring specificity is largely unknown.

We have focused on studying the wiring specificity of the fly olfactory system from the perspective of the second order PNs. Because lineage and birth order provide important information to determine where a PN should send its dendrites, it is likely that PNs of different glomerular classes express different combinations of transcription factors. A specific set of transcription factors might then direct the expression of a unique combination of cell surface receptors within PNs of a particular glomerular class, allowing their dendrites to choose a specific location in the antennal lobe and their axons to exhibit a specific terminal arborization pattern in higher olfactory centers. Indeed, we have recently found that a pair of POU domain transcription factors, Acj6 and Drifter, are differentially expressed in the two main PN lineages and regulate wiring specificity of PNs of these two lineages (Komiyama et al., 2003). While exploring other transcription factors that work together with the POU factors, we have started to examine cell surface receptors that dictate wiring specificity in the olfactory circuit.

Cadherins are Ca^{2+}-dependent cell adhesion proteins that are attractive candidates for regulating wiring specificity in the developing nervous systems. They are enriched in synaptic junctions, mediate synaptic adhesions, and have considerable molecular diversity (Shapiro and Colman, 1999). In a typical mammalian genome, more than 20 genes encode different "classic" cadherins (Yagi and Takeichi, 2000); in addition, families of protocadherins encode >50 proteins with variable extracellular domains (Wu and Maniatis, 1999). Such diversity has been proposed to function in the selection of specific synaptic partners and for stabilizing specific synaptic connections (Shapiro and Colman, 1999; Yagi and Takeichi, 2000). In *Drosophila*, N-cadherin shows expression predominantly in the nervous system (Iwai et al., 1997) and plays essential functions in axon patterning in the embryonic nervous system (Iwai et al., 1997) and in targeting specificity of photoreceptor axons (Lee et al., 2001). Recent genome analysis suggests that N-cadherin is alternatively spliced to generate eight distinct isoforms with variations in three pairs of exons encoding parts of the extracellular domain and the transmembrane domain (FlyBase; see also Iwai et al., 1997). In addition to N-cadherin, the fly genome contains a highly similar gene, *N-cadherin2*, located next to the *N-cadherin* genomic locus (FlyBase); a gene encoding E-cadherin, which is expressed primarily in epithelial cells including neural precursors (Dumstrei et al., 2003; Tepass et al., 1996; Uemura et al., 1996); and several other cadherin superfamily members (Hynes and Zhao, 2000).

Do cadherins play a role in wiring specificity of the

*Correspondence: lluo@stanford.edu

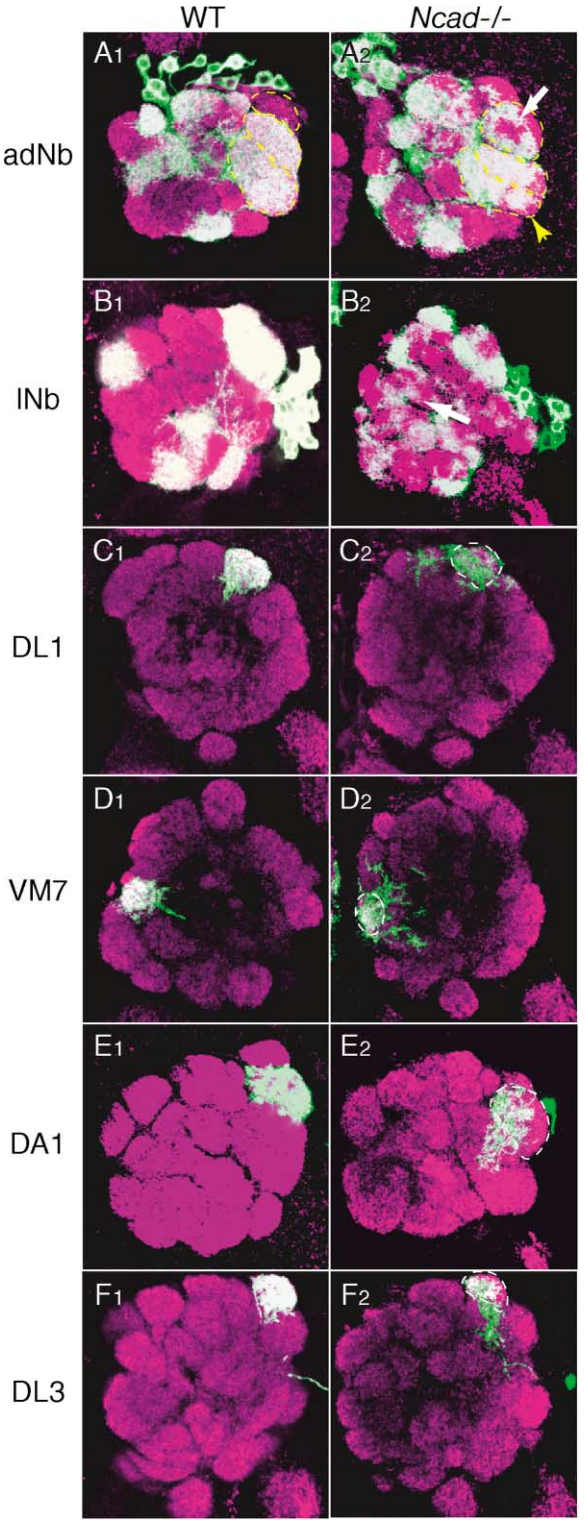

Figure 1. N-Cadherin Phenotype in Projection Neuron Dendrites

Representative confocal images of PN MARCM clones of wild-type (A_1–F_1) and *N-cadherin*$^{-/-}$ (A_2–F_2) highlighting their dendritic projection in the antennal lobe.

(A and B) Representative neuroblast clones ($n > 20$ for each category). Arrows in (A_2) and (B_2) indicate examples of ectopic dendritic innervation. Arrowhead in (A_2) points to the lack of complete innervation of VA1lm. Glomeruli DA1, VA1d, and VA1lm are outlined from top to bottom in (A_1) and (A_2), which are mounted from slightly different angles.

(C–F) Representative single-cell clones ($n > 50$ for DL1; $n \geq 6$ for other classes). The dashed white lines in (C_2)–(F_2) mark the boundaries of the presumed target glomeruli.

Unless indicated otherwise, all images in this and subsequent figures are maximum intensity Z projections of confocal stacks; dorsal is uppermost and medial is on the left. Similarly, unless indicated otherwise, brains are stained with anti-mouse CD8 antibody to label projection neurons of MARCM clones (green) and counterstained with anti-nc82 antibody to label the antennal lobe (magenta).

olfactory system? Do the various isoforms of N-cadherin contribute to this function? Here we examine the roles of *Drosophila* N-cadherin in the wiring of olfactory neural circuits, focusing primarily on its role in controlling the connectivity of projection neurons.

Results

To study cell-autonomous functions of candidate genes for their roles in PN wiring specificity, we used the MARCM strategy (Lee and Luo, 1999) to generate positively labeled homozygous mutant clones in an otherwise unlabeled and largely heterozygous genetic background. We focus our analysis on projection neurons that express GH146-GAL4, which accounts for ~90 of the estimated 150–200 PNs (Stocker et al., 1997). The majority of GH146-positive PNs (from here on referred to as PNs) are of the anterodorsal (adPNs) and lateral (lPNs) neuroblast lineages that innervate stereotypical, intercalated, yet nonoverlapping sets of glomeruli (Jefferis et al., 2001). These PNs can be visualized as neuroblast clones (Figures $1A_1$ and $1B_1$) or single-cell clones (Figures $1C_1$–$1F_1$) using MARCM. We tested strong loss-of-function mutants in a number of cadherin superfamily cell adhesion molecules including N-cadherin, E-cadherin, Flamingo, Fat, and Dachsous (Hynes and Zhao, 2000). The only mutant that shows a detectable phenotype in PN dendrite or axon patterning is *N-cadherin*, on which we will focus the rest of this study. We have exclusively used the allele *N-cadherin*^{M19}, which appears to be a complete loss-of-function allele: it contains a stop codon in the extracellular domain, is nearly protein null when assayed with an antibody against an extracellular epitope before the stop codon, and it behaves genetically as a null in embryonic nervous system patterning (Iwai et al., 1997).

N-cadherin is widely expressed in the olfactory system. It is concentrated in the developing adult-specific antennal lobe from early pupal stages, with contributions from both PN dendrites and, later on, ORN axons (Figure 2; Jefferis et al., 2004; Hummel and Zipursky, 2004 [this issue of *Neuron*]). It is also highly enriched in higher olfactory centers where PN axons terminate, including the entire mushroom body calyx and the lateral horn, throughout development and in the adult (data not shown).

N-Cadherin Is Required for Uniglomerular Targeting of PN Dendrites

When MARCM clones are induced in newly hatched larvae, neuroblast clones from anterodorsal and lateral

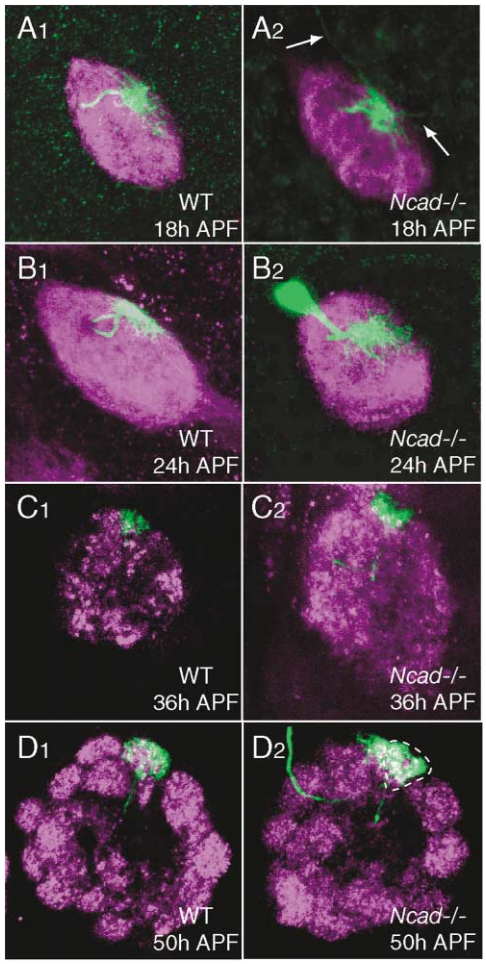

Figure 2. N-Cadherin Regulates Projection Neuron Dendritic Refinement during Development

Representative confocal images of dendrites of wild-type (A_1–D_1) and *N-cadherin*$^{-/-}$ (A_2–D_2) single-cell DL1 MARCM clones ($n \geq 4$) at different developmental stages as indicated (hours after puparium formation). The arrows in (A_2) indicate the dendritic processes shooting out of the antennal lobe. Pupal brains from 18 hr (A_1 and A_2) and 24 hr (B_1 and B_2) APF were stained with rabbit anti-GFP antibody in green to label MARCM clones and rat anti-N-cadherin antibody in magenta to label the developing antennal lobe. Some samples are unavoidably mounted at slightly different angles (e.g., B_1 versus B_2), contributing to seemingly different degree of dendritic spread.

lineages each include ~30–35 PNs, all of which are dedicated to the adult olfactory circuit; these adPNs and lPNs innervate approximately 13 and 12 glomeruli, respectively (Jefferis et al., 2001). Compared to wild-type neuroblast clones (Figures $1A_1$ and $1B_1$), PNs homozygous for the *N-cadherin*^{M19} allele (*N-cadherin*$^{-/-}$) target their dendrites to approximately the same stereotypical set of glomeruli appropriate for their lineage (Figures $1A_2$ and $1B_2$). However, several defects are evident. Dendrites targeted to a particular glomerulus are no longer restricted within the confines of that glomerulus; the general dendritic distribution is more diffuse compared with controls. As a consequence, glomeruli that are not appropriate for the lineage are often partially innervated (e.g., DA1 for adPNs as indicated by arrow in Figure $1A_2$). On the other hand, glomeruli appropriate for the lineage are often less fully occupied when compared with wild-type (e.g., VA1lm as indicated by arrowhead in Figure $1A_2$). There is also a noticeable distortion of glomerular pattern as revealed by staining for a neuropil marker using monoclonal antibody nc82 (magenta in all panels), although in most cases individual glomeruli can still be clearly identified.

To examine dendritic targeting at higher resolution, we analyzed single-cell clones. Our previous analyses have revealed that single-cell clones induced during the first 24 hr after larval hatching invariably belong to the DL1 class (Jefferis et al., 2001), allowing us to identify DL1 single-cell clones independent of the glomerular innervation pattern. We generated *N-cadherin*$^{-/-}$ and wild-type DL1 single-cell clones by heat shock induction of mitotic recombination shortly after larval hatching. A comparison of *N-cadherin*$^{-/-}$ and wild-type DL1 single-cell clones (Figure $1C_2$ versus $1C_1$) revealed that *N-cadherin*$^{-/-}$ DL1 PNs still target the majority of their dendrites to the DL1 glomerulus. However, unlike wild-type DL1 PNs (which target all their dendrites to the DL1 glomerulus), a significant fraction of dendrites in *N-cadherin*$^{-/-}$ PNs spread to several neighboring glomeruli with a preference for the glomerulus DL5, which is innervated by embryonic born PNs from the same adNb lineage (E.C. Marin and L.L., unpublished observation). At the same time, the density of dendritic mass within DL1 is reduced in *N-cadherin*$^{-/-}$ PN single-cell clones.

To analyze DA1 class of single-cell clones, we performed MARCM analysis using Mz19-GAL4, which labels three specific glomerular classes of PNs: VA1d and DC3 from the adNb lineage and DA1 from the lNb lineage (Jefferis et al., 2004). Therefore, lateral single-cell clones generated using Mz19-GAL4 will invariably belong to DA1 class. In *N-cadherin* mutant MARCM single-cell clones from the lateral lineage, the PN dendrites still target to DA1 but show significant spread to neighboring glomeruli (compare Figures $1E_1$ and $1E_2$). This phenotype is qualitatively similar to that of the DL1 single-cell clones.

To extend our studies of DL1 and DA1 PNs to other PN classes at single-cell resolution, we induced MARCM clones (examined with GH146-GAL4) at a late developmental stage (40 to 72 hr after larval hatching). Single-cell clones generated during this time window generally belong to a large number of glomerular classes besides DL1 (Jefferis et al., 2001). Although we have no independent molecular markers to distinguish most PN classes, we find that dendritic processes in the vast majority of single-cell clones tend to arborize mainly in a specific glomerulus. In most cases we could infer the glomerular class of single-cell PN clones by the entry of the main dendritic process to a glomerulus, with time of clone induction and lineage providing corroborating evidence. In all PN single-cell clones examined, the phenotypes are strikingly similar to that of DL1 and DA1: (1) a reduction of dendritic density in the major target glomerulus and (2) spreading of dendrites to a number of neighboring glomeruli. Figures 1D and 1F show examples of two different PN classes, VM7 PNs from the same anterodorsal lineage as DL1 and DL3 PNs from the lateral lineage as DA1.

Taken together, these data indicate that N-cadherin is not required for coarse targeting of PN dendrites to class-specific locations in the antennal lobe for at least two (DL1 and DA1) and likely all classes of PNs examined. Instead, N-cadherin is required by all PN classes examined to restrict their dendrites to a single target glomerulus.

Developmental Origin of N-Cadherin Dendritic Phenotypes

PN dendritic development has recently been characterized in detail (Jefferis et al., 2004). At 18 hr after puparium formation (18 hr APF), when pioneering axons of olfactory receptor neurons (ORNs) have just reached the periphery of the antennal lobe, PN dendrites already show substantial growth and patterning: PN dendrites occupy stereotypic locations in the antennal lobe such that a prototypical dendritic map has already formed in the absence of ORN axons. However, dendrites from individual PN classes still occupy a larger fraction of the antennal lobe at 18 hr APF compared to adult. Restriction of the dendritic field of individual PNs to single glomeruli occurs in the next 30 hr concomitant with invasion of ORN axons and maturation of glomeruli (as visualized by nc82 staining). Glial processes then start to invade the antennal lobe to wrap individual glomeruli from 50 hr APF (Figures $2A_1$–$2D_1$; Jefferis et al., 2004). Thus, PN dendritic development can be operationally separated into two stages. In the first stage (0–18 hr APF), PNs target their dendrites to an approximate location, establishing distinctive yet overlapping patterns of innervation in the antennal lobe independent of ORNs. In the second stage (18–50 hr APF), PN dendrites are refined to achieve uniglomerular innervation. This second stage of PN development could be influenced by ORN axons. At what stage is N-cadherin function required?

To address this question, we compared the morphology of *N-cadherin*$^{-/-}$ PNs with that of wild-type PNs during development in DL1 single-cell MARCM clones. We found that at 18 hr APF, *N-cadherin*$^{-/-}$ PNs target their dendrites to the same class-specific location as their wild-type counterparts in single-cell DL1 clones (Figure 2A). Because wild-type dendrites are still quite diffuse with numerous filopodial spikes at this stage, it is difficult to assess quantitatively whether *N-cadherin*$^{-/-}$ dendrites are more diffuse than in wild-type animals. However, we did notice one qualitative distinction: dendritic branches often shoot out of the developing antennal lobe in mutants (arrows in Figure $2A_2$; 4 out of 4 DL1 single-cell clones), which was not observed in any of the wild-type samples. As development proceeds, wild-type PNs gradually restrict their dendrites to innervate discrete glomeruli (Figures $2A_1$–$2D_1$), whereas *N-cadherin*$^{-/-}$ PN dendrites fail to fully refine and do not show uniglomerular innervation by 50 hr APF (Figures $2A_2$–$2D_2$). These observations indicate that N-cadherin is not essential for initial PN dendritic targeting, but rather is required for PN dendritic refinement.

Lack of Evidence for N-Cadherin Mediating ORN-PN Interaction

Cadherins have been postulated to play an important role in synaptic adhesion between pre- and postsynaptic neurons (Shapiro and Colman, 1999). Since substantial PN dendritic refinement occurs between 18 and 50 hr APF, after ORN axon arrival, ORN axons could play a role in this process. It is thus attractive to postulate that N-cadherin mediates adhesion between ORN axons and PN dendrites, thereby contributing to uniglomerular restriction of PN dendrites. To test this hypothesis, we examined the behavior of heterozygous (and phenotypically wild-type) PNs when ORNs are predominantly homozygous mutant for *N-cadherin*.

We used *eyeless-FLP* (*eyFLP*) in combination with a cell lethal mutant (Newsome et al., 2000) to generate large *N-cadherin*$^{-/-}$ ORN clones. *eyFLP* is expressed in antenna and maxillary palp precursors but not in the antennal lobe (Hummel et al., 2003). When *eyFLP* is used in combination with a cell lethal mutation in *trans* to the mutation of interest, 85%–90% of ORNs are homozygous for the mutation of interest (D. Berdnik and L.L., unpublished observations), presumably after FLP-mediated mitotic recombination because their siblings are homozygous for the cell lethal mutation and are thus eliminated (Newsome et al., 2000). To visualize dendritic projections of defined PN classes, we again made use of Mz19-GAL4, which is expressed in PNs innervating three glomeruli: DA1 and VA1d in the anterior antennal lobe (see Figure $3A_1$) and DC3 in the posterior (Jefferis et al., 2004). We found that, consistent with the important roles of N-cadherin in ORN axon targeting (Hummel and Zipursky, 2004), when the majority of ORNs are *N-cadherin*$^{-/-}$, there is a severe disruption of glomerular development as judged by nc82 staining. Glomerular borders are blurred and individual glomeruli are no longer identifiable (compare magenta in Figures $3A_1$ and $3A_2$). Despite this general perturbation, Mz19-positive PN dendrites still target to a dorsolateral region of the anterior part of the antennal lobe, where VA1d and DA1 glomeruli normally reside (Figure $3A_2$). However, because of the disruption of glomerular structure, it is impossible to judge the degree to which these dendrites are confined to their appropriate target glomeruli, although the dendrites appear more diffuse than in controls.

We then examined PN dendritic development when most ORNs are *N-cadherin*$^{-/-}$ at 50 hr APF; at this stage, wild-type PN dendrites have completed their uniglomerular refinement (Figures 2D and $3A_3$; Jefferis et al., 2004). We found that the dendrites of Mz19-positive PNs have refined normally even though ORNs are predominantly *N-cadherin*$^{-/-}$ (compare Figures $3A_4$ and $3A_3$), despite disruption of glomerular development as judged by nc82 staining. This experiment strongly suggests that N-cadherin in ORN axons is not essential for PN dendritic refinement, in contrast to its requirement in PNs for this process (Figure 2B). Rather, the diffuse appearance of Mz19-positive PN dendrites in adults but not 50 hr APF pupae suggests a function for ORNs in stabilizing PN dendrites after their initial refinement. Alternatively, this pattern could reflect an indirect consequence of antennal lobe disorganization when the majority of ORNs are devoid of N-cadherin.

We next tested whether disruption of N-cadherin in PNs would have an effect on ORN axon development. We generated *N-cadherin*$^{-/-}$ neuroblast clones in PNs by MARCM and visualized the development of a specific

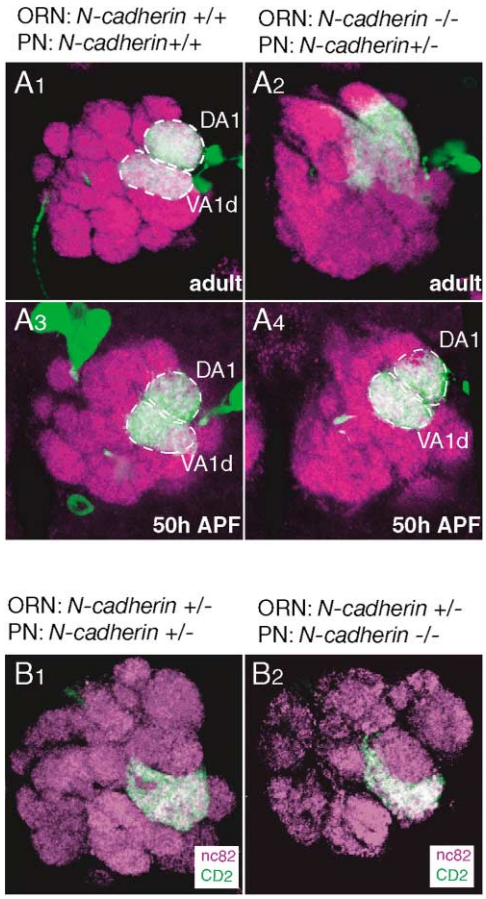

Figure 3. Test for N-Cadherin-Mediated Interaction between PN Dendrites and ORN Axons

(A) Effect of *N-cadherin*$^{-/-}$ ORN axons on PN dendritic morphology. Unlabeled wild-type (A_1 and A_3) and *N-cadherin*$^{-/-}$ (A_2 and A_4) ORN clones were generated with Eyeless promoter driven expression of the FLP recombinase. A subset of PNs were visualized with Mz19-GAL4 driven expression of UAS-mCD8-GFP. Brains from adults (n = 10 for both A_1 and A_2) and 50 hr APF (n = 14 and 8 for A_3 and A_4, respectively) were examined for PN dendritic morphology and gave consistent results as shown in these representative images.

(B) Effect of *N-cadherin*$^{-/-}$ PN dendrites on axon projection from OR-47b ORNs. Axonal morphologies of ORNs expressing Or47b were compared in brain hemispheres with no clones (B_1, n = 15) and with both *N-cadherin*$^{-/-}$ adNb and vNb PN MARCM clones (B_2, n = 5). Axonal projections of Or47b ORNs were labeled by the Or47b-CD2 transgene and visualized with anti-CD2 antibody (green, becomes white when overlay over nc82 staining in magenta).

class of ORN axon using a transgene in which the Or47b promoter drives CD2 expression (see Experimental Procedures). Axons from ORNs expressing the Or47b odorant receptor normally converge onto the VA1lm glomerulus (Figure $3B_1$; Vosshall et al., 2000); PNs innervating VA1lm belong to both anterodorsal and ventral lineages (Marin et al., 2002). When we generated heat shock-induced *N-cadherin*$^{-/-}$ MARCM clones at early larval stages, in about 10% of cases we generated an anterodorsal and a ventral neuroblast clone in the same brain hemisphere. In the brain hemispheres containing double neuroblast clones, all the GH146-positive PNs innervating VA1lm are *N-cadherin*$^{-/-}$ and show severe dendritic overspill (data not shown). However, the axonal arborization of Or47b-expressing ORNs, as visualized by anti-CD2 staining, is restricted to the VA1lm glomerulus (Figure $3B_2$, green), indistinguishable from wild-type controls (Figure $3B_1$). These data do not support the notion that N-cadherin-mediated ORN-PN interactions play a role in ORN axon targeting in the antennal lobe, at least for the Or47b class of ORNs. Moreover, since the mutant VA1lm PN dendrites spread outside VA1lm, whereas the ORN axons are not affected, ORNs are unlikely to use their target PN dendrites as a primary cue to determine their axon targeting.

Evidence that N-Cadherin Mediates Dendro-Dendritic Interactions among PNs

We have demonstrated that N-cadherin is required in PNs before 50 hr APF to restrict their dendritic targeting. Since N-cadherin expression in ORN axons is not required in this dendritic refinement process (Figure 3A) and glial processes do not invade the antennal lobe until after 50 hr APF (Jefferis et al., 2004), we hypothesized that N-cadherin may mediate homophilic interactions among PN dendrites.

To test this hypothesis, we used a strategy called reverse MARCM (Lee et al., 2000). In this strategy, the tubulin-Gal80 transgene is introduced on the same chromosome arm as the *N-cadherin* mutant, distal to the FRT site. In this way, the GFP-labeled cells are now homozygous wild-type, whereas the invisible twin spot of the labeled clone (the sister cell of the labeled clone after mitotic recombination, and all its progeny) is *N-cadherin*$^{-/-}$. We induced mitotic recombination at an early larval stage (0–8 hr after larval hatching). At this stage, all neuroblasts are arrested for their proliferation except for 4 neuroblasts that contribute to the mushroom body neurons and a lateral neuroblast, giving rise to local interneurons of the antennal lobe and lateral PNs (Ito and Hotta, 1992; Stocker et al., 1997). Despite the arrest of cell division in the anterodorsal neuroblast, FLP induction via heat shock can still produce clones (single-cell clones are invariably DL1 from 0 to 24 hr after larval hatching), presumably because the arrest occurs at the G2 stage when duplicated chromosomes can undergo recombination. Therefore, if we induce reverse MARCM clones in early larvae and generate a labeled single-cell DL1 clone that is homozygous wild-type, the invisible twin spot will inevitably be a *N-cadherin*$^{-/-}$ neuroblast clone containing all the later born DL1 PNs as well as later-born anterodorsal PNs of other glomerular classes (Figure 4A; Jefferis et al., 2001). We reasoned that if N-cadherin mediates homophilic interactions among PN dendrites, then labeled *N-cadherin*$^{+/+}$ DL1 PNs developing in an environment in which neighboring dendrites (and in particular other DL1 PN dendrites) are *N-cadherin*$^{-/-}$ might exhibit dendritic spillover phenotypes similar to those of *N-cadherin*$^{-/-}$ DL1 clones in the "forward" MARCM setting (Figure $1C_2$).

Indeed, we observed that DL1 reverse MARCM clones show significant dendritic spillover into neighboring glomeruli including DL5 and DL2 (Figures 4C and 4D, compare with Figure 4B). Moreover, in 6/16 clones examined, there are also dendritic processes shooting out of the antennal lobe (arrow in Figure 4D), a phenotype never

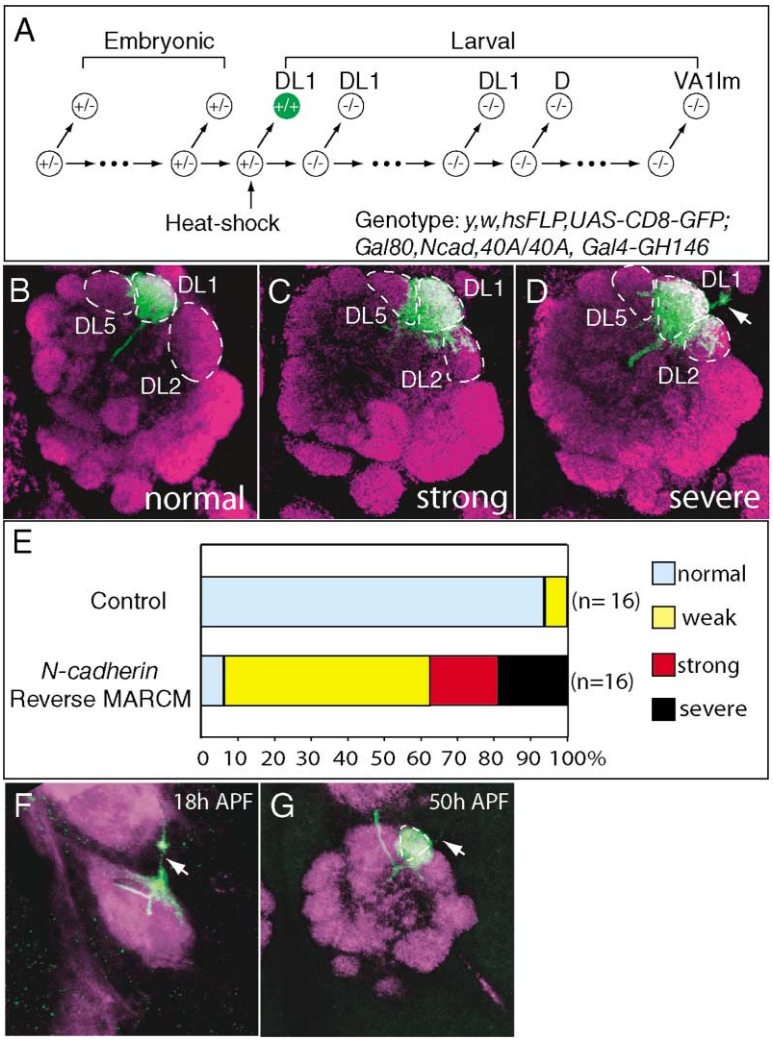

Figure 4. N-Cadherin Mediates Dendro-Dendritic Interactions among Projection Neurons

(A) Schematic diagram of the method used to generate DL1 single-cell reverse MARCM clones. Note that the green GFP-labeled single cell is the only DL1 PN that is wild-type for *N-cadherin*.

(B–E) Characterization of *N-cadherin* DL1 reverse MARCM phenotype in adults, showing representative images of normal (B), strong overspill (C), and severe overspill (D) dendritic phenotypes of DL1 reverse MARCM clones. Dashed lines in (B)–(D) mark the glomerular boundary as judged by nc82 staining (magenta). The arrow in (D) indicates a dendritic process shooting out of the antennal lobe. Quantifications of DL1 phenotypes of control and N-cadherin reverse MARCM clones are shown in (E).

(F and G) Representative images of *N-cadherin* reverse MARCM phenotypes at 18 hr (F) and 50 hr (G) APF. The arrows in (F) and (G) indicate dendritic processes shooting out of the antennal lobe. 18 hr APF brains were stained with anti-GFP antibody (green) and anti-N-cadherin antibody (magenta).

observed in wild-type clones. To quantitatively assess the phenotype, we performed a blind scoring of DL1 control and reverse MARCM clones. We scored the dendritic overspill of DL1 clones as one of four classes: normal, weak, strong, or severe overspill. This blind test revealed that 15/16 wild-type DL1 clones fell into the normal category, whereas 15/16 reverse MARCM clones fell into weak (9), strong (3), or severe (3) overspill categories (Figure 4E). Further, we found that the *N-cadherin* reverse MARCM phenotypes occur early in pupal development. At 18 hr APF, we observed dendritic processes shooting out of the antennal lobe in three of the six samples (Figure 4F), a phenotype similar to forward MARCM (Figure 2). At 50 hr APF, overspill phenotypes similar to the strong or severe phenotypes in the adults were observed in 9 of the 19 samples examined (Figure 4G). Thus, the onset of the reverse MARCM phenotype coincides with dendritic refinement (Figure 2).

In summary, *N-cadherin* mutant dendrites in an otherwise normal environment overspill beyond their glomerular target (Figure 1); wild-type dendrites in an environment where some surrounding PN dendrites are mutant for *N-cadherin* also overspill beyond their glomerular target (Figure 4); both these phenotypes arise during dendritic refinement. The simplest interpretation is that N-cadherin mediates dendro-dendritic interactions that allow individual PNs to refine their dendritic targeting to single glomeruli (see Discussion).

N-Cadherin Controls Stereotypical Terminal Arborization of PN Axons

We next investigated N-cadherin's function in PN axon development by examining *N-cadherin*$^{-/-}$ neuroblast and single-cell MARCM clones (Figure 5). We found that in mutant neuroblast and single-cell clones (compare Figures $5A_2$–$5C_2$ with $5A_1$–$5C_1$), *N-cadherin*$^{-/-}$ PN axons follow the correct trajectory and arborize in the mushroom body calyx and the lateral horn, indicating that N-cadherin is not required for PN axon growth and guidance to higher olfactory centers. At the target regions, the axon arborizations of *N-cadherin*$^{-/-}$ adNb clones appear to be less extensive in the lateral horn, but more profuse in the mushroom body calyx, than in wild-type animals (compare Figures $5A_2$ with $5A_1$), suggesting that N-cadherin may function in PN axon terminal arborization.

To study the effect of N-cadherin on PN axons at single-cell resolution, we examined the axonal arboriza-

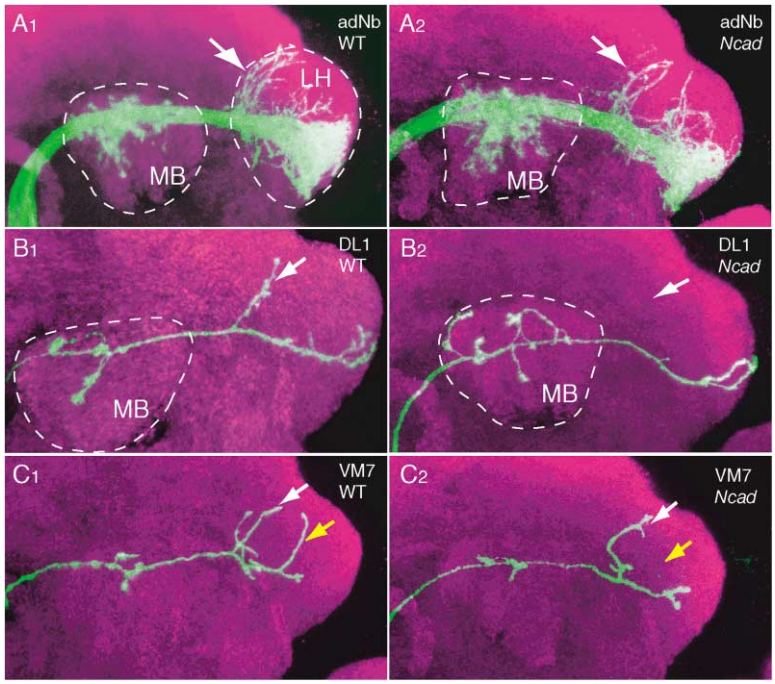

Figure 5. N-Cadherin Phenotypes in Projection Neuron Axons

Representative confocal images of axons of wild-type (A_1–C_1) and *N-cadherin*$^{-/-}$ (A_2–C_2) PN MARCM clones. A_1 and A_2 show antero-dorsal neuroblast clones. Dashed lines circle the mushroom body calyx (MB) and lateral horn region (LH) as judged by nc82 staining. The arrows in (A_1) and (A_2) indicate the dorsal axon bundles of the adNb. (B_1) and (B_2) show axons of single-cell clones of DL1 PNs. Arrows indicate the presence (B_1) and absence (B_2) of the dorsal branch. See Figures 7E and 7F for MB branch quantification. (C_1) and (C_2) show axons of VM7 PNs. The white and yellow arrows indicate the medial and lateral dorsal branches, respectively.

tion pattern of DL1 single-cell clones in the lateral horn. Wild-type DL1 single-cell clones exhibit stereotypical axonal branching patterns in the lateral horn area, characterized by the presence of a major dorsal branch and a lateral branch (Figure 5B_1; Marin et al., 2002). In *N-cadherin*$^{-/-}$ DL1 single-cell clones, however, the dorsal axon branch is invariably missing, whereas the lateral branch is not affected (Figure 5B_2). This phenotype is 100% penetrant ($n > 50$).

To ascertain whether loss of N-cadherin affects other classes of PN axons that project dorsally in the lateral horn, we selected among single-cell clones generated during the mid-larval period (see Figures 1D and 1F) samples for which (1) we can assess the glomerular class by the major dendritic branch entry point to the glomerulus, (2) we have several examples for a particular class, and (3) lateral horn arborization includes stereotypical dorsal branch(s). PNs of the VM7 class fulfill these criteria; every wild-type single-cell clones we examined ($n = 15$) has two dorsal branches, one closer to the medial edge of the lateral horn (as the dorsal branch in DL1) and one in the middle of the lateral horn (Figure 5C_1; Marin et al., 2002). Intriguingly, only the more lateral of the two dorsal branches is missing in *N-cadherin*$^{-/-}$ VM7 PNs ($n = 5/5$), whereas the more medial dorsal branch and the main lateral branch are not affected (Figure 5C_2). These results suggest that N-cadherin affects a highly specific subset of PN dorsal axon branches in the lateral horn.

In the mushroom body calyx, wild-type PNs usually exhibit a few collateral branches that end in large boutons likely to be synapses (Yasuyama et al., 2002). *N-cadherin*$^{-/-}$ DL1 clones appear to have more axon terminals and branches than wild-type (Figure 5B_2 compared with Figure 5B_1). We quantified the axon branches and terminals in the mushroom body calyx of wild-type and *N-cadherin*$^{-/-}$ single-cell clones of the DL1 class (of which we have sufficient numbers). We found a 50% increase in the number of axon terminals in the mushroom body calyx of *N-cadherin*$^{-/-}$ DL1 clones compared with wild-type (Figure 7E). This change is not due to an increase of primary branches, but rather is caused by a marked increase of the number of higher order branches (Figure 7F). These data suggest that N-cadherin plays a role in restricting high-order axon terminal branching and likely the total number of synaptic connections made by PNs in the mushroom body calyx.

N-Cadherin Is Required for Dorsal Axon Branch Stability in the Lateral Horn

To investigate the mechanisms of axon arborization defects in *N-cadherin* mutant PNs, we compared the developmental time course of PN terminal arborization in wild-type and single-cell DL1 clones. The dorsal axon branch in DL1 PNs is formed by a process of collateral extension (Jefferis et al., 2004). We found that as in wild-type, dorsal axon branches formed normally in *N-cadherin*$^{-/-}$ DL1 clones by 36 hr APF in all four samples examined (Figure 6A_2, compared with 6A_1). However, these dorsal axon branches are not seen in pupae at 42 or 50 hr APF (Figures 5B and 5C; $n = 3$ and 6, respectively). These observations indicate that N-cadherin does not affect the initial extension of the dorsal axon branches, but rather functions in stabilizing them.

We also tried to determine the origin of the exuberant branching phenotype of *N-cadherin* mutant axons in the mushroom body calyx. The miniature scale and numerous filopodia-like structures of DL1 collaterals at pupal stages made it impossible for us to quantitatively assess the axon branching phenotype in the mushroom body calyx during development. However, it appears that there are more axon branches in mutant than in wild-type animals from 36 hr APF (Figure 6A). This phenotype persists during later pupal stages (Figures 6B and 6C).

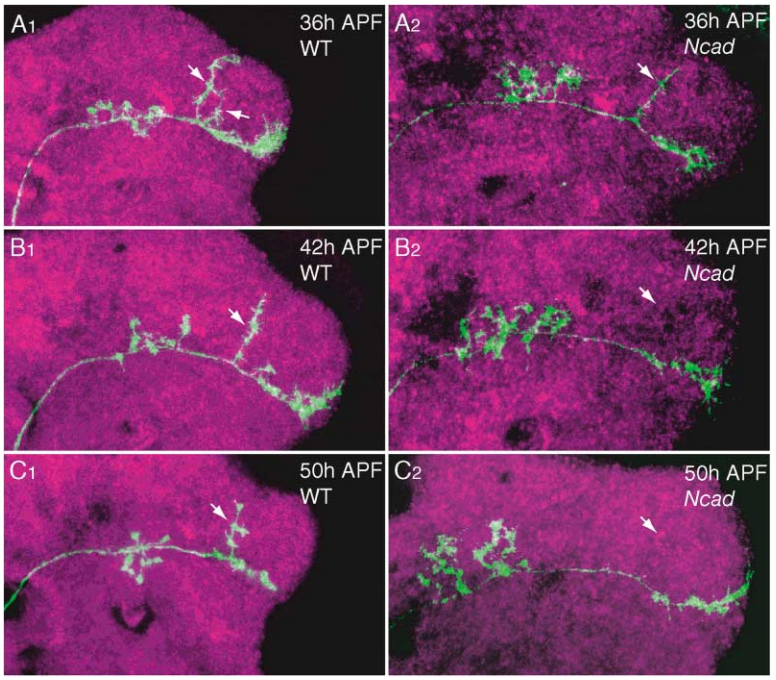

Figure 6. N-Cadherin Controls Axonal Branch Stability in DL1 PNs

Representative images of axons of wild-type (A_1–C_1) and *N-cadherin*$^{-/-}$ DL1 (A_2–C_2) single-cell clones at 36 hr (A), 42 hr (B), and 50 hr (C) APF. Note the presence of two dorsal branches in wild-type DL1 clones at 36 hr APF (arrows in A_1). Also note in the *N-cadherin* mutant clones the dorsal branches (indicated by the arrows) are present at 36 hr APF (A_2) but are missing at 42 hr and 50 hr APF (B_2 and C_2).

This observation suggests that unlike the axonal phenotype in the lateral horn, the branching phenotype in the mushroom body calyx may arise at an earlier stage during development. In the first case, N-cadherin appears to play a late stabilization role, while in the calyx N-cadherin may be required from early stages to limit high-order branching.

Transgenic Expression of a Single Isoform of N-Cadherin Rescues All Phenotypes

The N-cadherin locus in the *Drosophila* genome potentially encodes eight different protein isoforms via alternative mRNA splicing (FlyBase). Specifically, each of exons 7, 13, and 18 has two alternative forms, namely 7a and 7b, 13a and 13b, and 18a and 18b, with exons 7 and 13 corresponding to extracellular cadherin repeats and exon 18 corresponding to the transmembrane domain. To test whether multiple isoforms are required for N-cadherin function in PN dendritic and axonal terminal arborization, we expressed a transgene encoding one particular isoform, N-cadherin (7a, 13a, 18a) (Iwai et al., 1997), in *N-cadherin* null mutant PNs to see to what extent this isoform could rescue the different mutant phenotypes. This experiment is possible because, in addition to its ability to generate positively labeled clones of mutant or wild-type PNs, MARCM can be used to express transgenes only in those same labeled PNs.

We first tested whether MARCM expression of UAS-N-cadherin (7a, 13a, 18a) in labeled wild-type PNs would generate any phenotypes. In both neuroblast and single-cell DL1 clones, expression of UAS-N-cadherin (7a, 13a, 18a) does not result in detectable phenotypes in dendrites (Figures $7A_1$–$7C_1$). It also does not cause changes in axonal branches in the mushroom bodies (Figure 7E). However, an interesting phenotype can be seen in axons of single-cell DL1 clones in the lateral horn. In 47% of the samples (n = 17), we observed that instead of the normal one dorsal axon branch, there were two dorsal branches in the lateral horn area (Figure $7D_1$). This phenomenon was also occasionally observed in wild-type DL1 single-cell clones during pupal stages, but never in adult (data not shown; Jefferis et al., 2004). This phenotype is consistent with the idea that N-cadherin stabilizes the dorsal axon branches in the lateral horn—perhaps a higher level of N-cadherin can stabilize branches that would otherwise be transient.

Remarkably, when N-cadherin (7a, 13a, 18a) was introduced into *N-cadherin*$^{-/-}$ mutant MARCM clones, we found that PN phenotypes were rescued in all three structures (antennal lobe, mushroom body calyx, and lateral horn). In both adNb and lNb mutant clones expressing UAS-N-cadherin (7a, 13a, 18a), PN dendrites are restricted to the appropriate sets of glomeruli (Figures $7A_3$ and B_3, compare with Figures $7A_2$ and B_2). In single-cell DL1 clones, N-cadherin (7a, 13a, 18a) expression is sufficient to restore wild-type DL1 uniglomerular dendritic innervation (Figure $7C_3$, compare with Figure $7C_2$). The missing dorsal axon branch phenotype in the lateral horn area is also restored (Figure $7D_3$, compare with Figure $7D_2$). Finally, the numbers of axonal terminals and branches in the mushroom body calyx are also reduced toward wild-type values (Figures 7E and 7F). These data indicate that diverse N-cadherin isoforms are not necessary for PN dendritic targeting in the antennal lobe, for restricting high order axon terminal branching in the mushroom body, or for stabilizing highly specific axon terminal branches in the lateral horn.

These rescue experiments also verify that the MARCM phenotypes reported in this study are caused by the mutation in the *N-cadherin* gene, rather than potential other background mutations on the same chromosomal arm. In addition, since the transgene is only expressed in labeled neurons, these rescue experiments rule out the possibility that the phenotypes observed in MARCM

experiments are caused by nonautonomous effects of N-cadherin loss in unlabeled mutant clones of cells that do not express GH146-GAL4.

Discussion

N-Cadherin and Synaptic Specificity

Cadherin superfamily members in vertebrates have been proposed to play important roles in regulating the specificity of synaptic connections in the developing nervous system, based on their expression patterns, synaptic localization, selective adhesive properties, and molecular diversity (Shapiro and Colman, 1999; Yagi and Takeichi, 2000). *Drosophila* N-cadherin has been proposed to play similar functions in the wiring of the visual system (Lee et al., 2001). Given the complex wiring problem in the olfactory system, cadherins are attractive candidates for cell surface proteins involved in selecting synaptic partners between different classes of ORNs and PNs. Indeed, *Drosophila* N-cadherin is highly expressed in the antennal lobe with contributions from both ORNs and PNs (Jefferis et al., 2004; Hummel and Zipursky, 2004). However, the genetic analyses described here do not support an instructive role for N-cadherin in determining olfactory wiring specificity in the antennal lobe.

Developmental studies reveal that the dendrites of *N-cadherin* mutant PNs occupy the same positions as their wild-type counterparts during early pupal development, arguing against a function for N-cadherin in initial dendritic targeting. Furthermore, *N-cadherin*$^{-/-}$ dorsal and lateral neuroblast clones largely preserved their dendritic innervation pattern. It remains possible that N-cadherin may function in determining individual PN glomerular choices within either the dorsal or lateral neuroblast lineage. However, analysis of single-cell clones of DL1 and DA1 class (of which we have independent criteria to verify their identities) argues against this possibility. On the other hand, the dendritic overspill phenotype is observed in every *N-cadherin*$^{-/-}$ single-cell clones, supporting a permissive role of N-cadherin in determining connection specificity in the antennal lobe. Analysis of the role of N-cadherin in ORNs also does not support a major instructive role in target selection of ORN axons (Hummel and Zipursky, 2004).

The fact that the *N-cadherin* locus encodes eight alternatively spliced isoforms makes it attractive to suppose that this molecular diversity is used for selective synaptic adhesion, thereby contributing to synaptic specificity. Yet we have shown that UAS-GAL4-mediated transgene expression of a single isoform is sufficient to rescue dendritic overspill phenotypes of all classes of PNs examined. This observation suggests that differential expression of *N-cadherin* at the level of transcription or alternative splicing is not required for PN dendritic targeting specificity.

At present we cannot rule out the possibility that N-cadherin plays an instructive role in determining targeting specificity of a subset of PNs that we have not analyzed (for instance GH146-negative PNs). It is also possible that N-cadherin may play a role in connection specificity in higher olfactory centers, especially in the lateral horn (see below).

Dendro-Dendritic Interaction in Restricting Dendritic Targeting: A Novel Function for N-Cadherin

Our study nevertheless has uncovered an important and novel function for N-cadherin in restricting dendritic targeting to single glomeruli. Every PN class we examined exhibited a remarkably similar phenotype: instead of dendrites of a single PN targeting to a single glomerulus, dendrites from *N-cadherin* mutant PNs spread to neighboring glomeruli. Developmental studies revealed a major function of N-cadherin in dendritic refinement. In wild-type animals, dendrites from a single PN initially occupy a proportionally larger area of the antennal lobe, presumably overlapping with dendrites of other PN classes. They then refine their dendritic domain to single glomeruli by 50 hr APF, concomitant with glomerular maturation (Figure 2; Jefferis et al., 2004). *N-cadherin* mutant dendrites initially occupy dendritic domains of roughly similar size, but they then fail to restrict their domains to a single glomerulus.

Dendritic refinement of second order olfactory neurons appears to be a common feature in both flies and mammals. Mammalian mitral/tufted cells, equivalent to PNs, also send their apical dendrites into several glomerular structures during early development, subsequently refining to a single glomerulus (Malun and Brunjes, 1996). The mechanism of this refinement is unclear. Interestingly, loss of odor-evoked neuronal activity of ORNs does not affect mitral cell dendritic refinement (Lin et al., 2000). Likewise, *Drosophila* PN dendritic refinement occurs before any OR receptor expression and before morphologically mature synapses are detected in the antennal lobe (Devaud et al., 2003), suggesting an activity-independent process.

What kind of cell-cell interactions does N-cadherin mediate during PN dendritic refinement? Previously, N-cadherin has been proposed to mediate axonal target selection in the visual system of *Drosophila* (Lee et al., 2001). During development, PN dendritic refinement coincides with ORN axonal invasion into the antennal lobe; N-cadherin is expressed in both ORNs and PNs at this time. Based on these observations, it is attractive to hypothesize that N-cadherin mediates homophilic interactions between ORN axons and PN dendrites to refine neural processes. However, we did not find any positive evidence for N-cadherin-mediated interaction between ORN axons and PN dendrites in PN dendritic refinement. Rather, the reverse MARCM analysis demonstrates that N-cadherin in other PNs of the same lineage, including PNs that occupy the same glomerulus, is required for the uniglomerular targeting of wild-type PNs.

What cellular mechanisms could explain both the autonomous and nonautonomous effects of N-cadherin in uniglomerular targeting? The simplest model is that N-cadherin expressed on the surface of PN dendrites confers proper adhesiveness to the dendrite during and after the initial targeting event. Loss of N-cadherin results in reduced cell adhesion, allowing dendrites to more easily invade the neighboring glomeruli or shooting out of the confines of the antennal lobe. The non-cell-autonomous effect of N-cadherin revealed by the reverse MARCM analysis suggests that their interaction partners are dendrites of other PNs, most likely of the same class and thereby occupying the same general

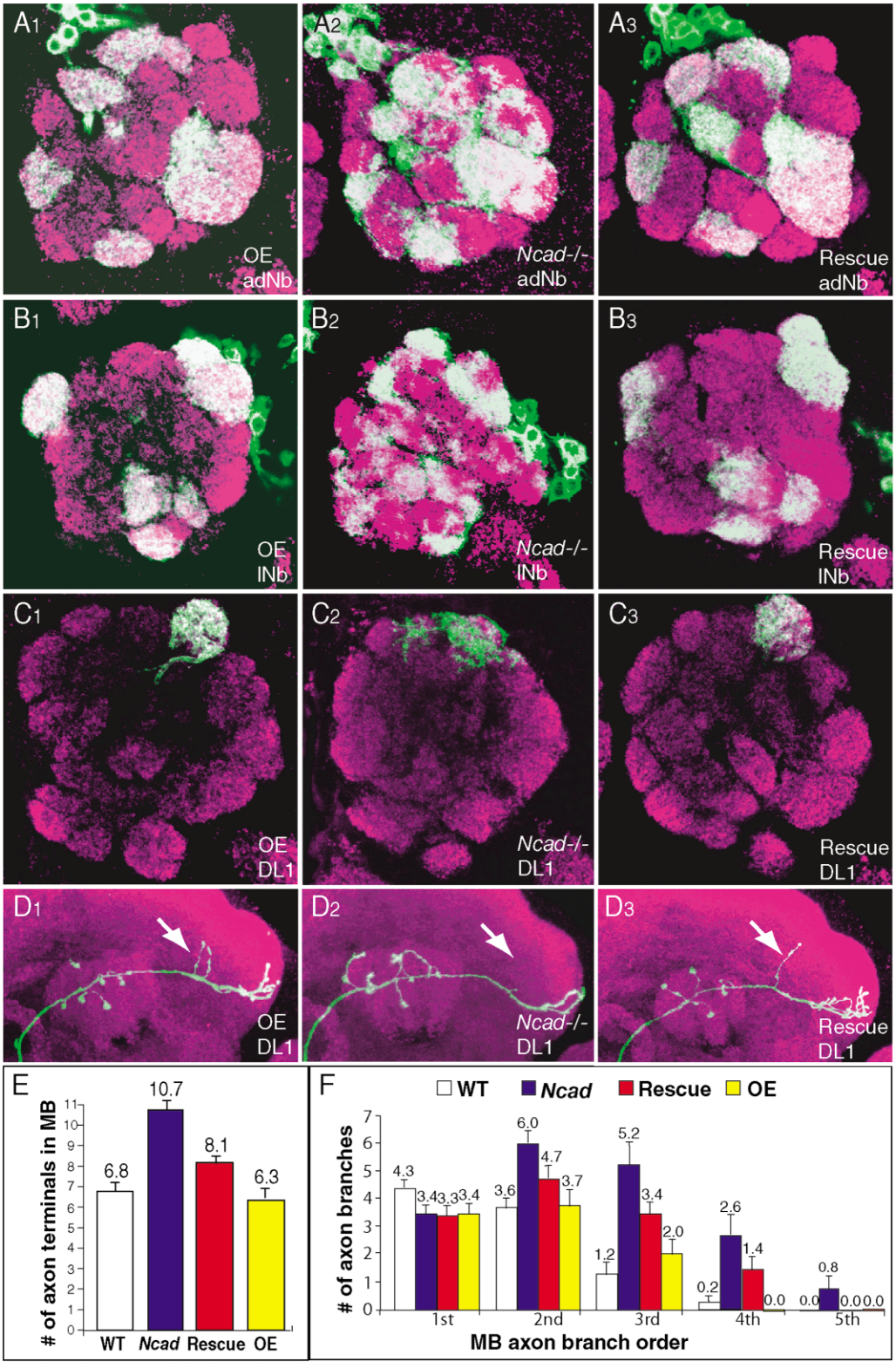

Figure 7. Transgene Expression of One Isoform Rescues *N-cadherin* Null Phenotypes in PNs

(A–D) Representative images of MARCM expression of UAS-N-cadherin (7a, 13a, 18a) in wild-type (A_1–D_1, OE for overexpression) and *N-cadherin* mutant (A_3–D_3, Rescue) PNs, compared with representative images of *N-cadherin*$^{-/-}$ PNs (A_2–D_2, *Ncad*$^{-/-}$). adNb (A_1–A_3), lNb (B_1–B_3), and DL1 single-cell (C_1–C_3) dendrites are shown. (D_1)–(D_3) show DL1 axons. n ≥ 10 in each panel. Arrows in (D_1) and (D_3) indicate the dorsal branches in the lateral horn. Note two dorsal axon branches are present in DL1 single-cell clones overexpressing the N-cadherin (7a, 13a, 18a) transgene (D_1).

domain. In this scenario, direct PN dendrite-dendrite interaction mediated by N-cadherin contributes to confining dendrites to individual glomeruli.

Other alternative scenarios are less likely. For instance, the reverse MARCM phenotype could be explained if altered PN patterning as a result of the unlabeled mutant neuroblast clones leads to altered ORN axons, which then indirectly affect the labeled wild-type PN. However, at least at the VA1lm glomerulus, we show that altered PN dendritic patterning does not result in a corresponding alteration of ORN axon arborization.

Since N-cadherin is expressed in all PN classes, it must work together with other cell surface proteins eventually to refine dendrites to their class-specific glomeruli. Some of these cell surface proteins may allow dendrites to be targeted to their appropriate spatial locations; others may mediate repulsive interactions among dendrites of different PN classes.

Implications for Cellular Interactions in the Construction of the Olfactory Circuit in the Antennal Lobe

We have recently proposed, based primarily on the developmental timing of PN dendritic patterning and ORN axon arrival, as well as studies of cellular constituents of the developing antennal lobe, that PN-PN interactions are utilized in creating a prototypic dendritic map before the arrival of ORN axons (Jefferis et al., 2004). Furthermore, as functional studies from mammals to moths suggest an autonomous role for ORNs in organizing glomerular pattern, we propose that ORN axons and PN dendrites may be capable of generating independent maps; ORN-PN interaction would then enable the registration of the two maps with one another (Jefferis et al., 2004). Analysis of the N-cadherin mutant phenotype and the interaction between mutant ORNs or PNs lends support to these hypotheses. First, we show that PN-PN interactions do occur and are essential at least for the uniglomerular targeting of dendrites. Second, the fact that dendritic overspill of PNs does not result in a corresponding ORN axon overspill supports the view that ORNs deploy targeting strategies independent of their future postsynaptic partners. At the same time, disruption of N-cadherin in ORNs does not affect the initial dendritic refinement of those neurons. It is possible that further ORN-PN interaction during the synapse maturation period could play a stabilizing role in the maintenance of synaptic connections, possibly explaining why disruption of N-cadherin in ORNs results in a more diffuse dendritic projection in adult.

Diverse Functions of N-Cadherin in a Single Type of Neuron

Our analysis has revealed that N-cadherin has diverse functions in a single type of neuron, olfactory projection neurons. In addition to its important roles in restricting the dendrites of each PN to a single glomerulus in the antennal lobe, N-cadherin is required for PN axon terminal arborization in both the mushroom body and the lateral horn. Do these diverse functions of N-cadherin reflect local actions of N-cadherin in these three sites, or could N-cadherin directly act in one site, with the phenotypes in other sites being secondary consequences due to intraneuronal communication? Several lines of evidence support the notion that N-cadherin acts locally and independently in PN dendrites and axons. First, N-cadherin is highly expressed in all three sites. Second, based on developmental analysis of the mutant phenotype, N-cadherin is required in overlapping time windows in these three sites. For instance, the antennal lobe phenotype suggests a continuous role of N-cadherin from before 18 hr APF to close to 50 hr APF, whereas its function in the lateral horn for DL1 PNs appears to be at 36–42 hr APF. The lack of clear-cut sequential actions makes the intraneuronal communication model less likely. Lastly, N-cadherin affects the dendrites of all classes of PNs but the axons of only a subset of PNs. For instance, although *N-cadherin* mutant DA1 single-cell clones exhibited dendritic phenotypes, the highly specific targeting of lateral horn terminal arborization to the anterior corner for the DA1 PN (Marin et al., 2002) was unaffected in *N-cadherin* mutant (data not shown). Such uncoupling argues against the intraneuronal signaling model.

Interestingly, axonal phenotypes in the two higher order olfactory centers appear qualitatively different. In the lateral horn, where PN axon terminal arborization is highly stereotyped according to glomerular class (Marin et al., 2002; Wong et al., 2002), we observed a strikingly specific perturbation of selective terminal branches in two classes of PNs. Developmental studies clearly demonstrate that N-cadherin affects lateral horn axon terminal branch stability, rather than its initial growth. This represents, to our knowledge, the first demonstration of selective stabilization of terminal branches mediated by a cadherin, which may well be important in establishing the specificity of synaptic connection of PN axons with their postsynaptic targets. Because of the lack of knowledge about the postsynaptic neurons and their dendritic fields in the lateral horn, the significance of loss of particular branches in synaptic specificity shall await future investigations. Finally, it was previously shown that the DL1 dorsal axon branch was also specifically disrupted in PNs deprived of the POU transcription factor Acj6 (Komiyama et al., 2003). Interestingly, these ultimately similar phenotypes are mechanistically distinct: Acj6 affects dorsal branch formation, whereas N-cadherin affects its stabilization.

The axonal branching pattern of PNs in the mushroom body is considerably less stereotyped than that in the

(E) Quantification of the number of axon terminals in the mushroom body calyx in DL1 single-cell clones. t tests: wt versus *Ncad*, $p = 0.0005$; *Ncad* versus Rescue, $p = 0.0012$; wt versus Rescue, $p = 0.0176$.

(F) Quantification of axon branching order of DL1 single-cell clones in mushroom body calyx. A first order axon branch is defined as a branch that branches out from the main PN axon tract, and a second order axon branch is defined as an branch that branches out from a first order axon branch, etc.

In (E) and (F), error bars represent standard error of the mean. wt, wild-type ($n = 10$); *NCad*, *N-cadherin* mutants ($n = 10$); Rescue, MARCM expression of UAS-N-cadherin (7a, 13a, 18a) in *N-cadherin* mutant PNs ($n = 10$); OE, MARCM overexpression of UAS-N-cadherin (7a, 13a, 18a) in wild-type PNs ($n = 7$).

lateral horn in wild-type animals (Marin et al., 2002). Here, at least for one class of PNs (DL1), N-cadherin functions to restrict exuberant higher-order branches, in contrast to its role in stabilizing selected branches in the lateral horn for the same class of PNs.

It is possible that that N-cadherin-mediated adhesion is differentially interpreted in different cellular contexts for the specific purposes. Mechanistically, the diverse functions of N-cadherin could be accomplished by N-cadherin working together with different partners at the cell surface or utilizing different intracellular signaling pathways. At the cell surface, a Robo-mediated inhibition of N-cadherin function has recently been proposed (Rhee et al., 2002). Intracellularly, the cytoplasmic domains of classic cadherins interact with β-, γ-, and δ-catenins (Yap et al., 1997). Components of Rho GTPase pathways have also been implicated in regulating cadherin-mediated cell-cell adhesions (Kaibuchi et al., 1999). The differential distribution of these cell surface partners and intracellular signaling components in different cellular compartments may explain the different actions of N-cadherin. While the molecular mechanisms await further investigations, our study along with the companion study in this issue of *Neuron* (Hummel and Zipursky, 2004) underscores the pleiotropic functions of this important class of cell adhesion proteins in multiple aspects of olfactory circuit assembly.

Experimental Procedures

Clonal Analysis

Applications of MARCM strategy were as described previously (Lee and Luo, 2001). MARCM clones were induced by 1.5 hr, 37°C heat shocks at either 0–18 hr after larval hatching or 40–72 hr after larval hatching. The genotypes of flies for various experiments are as follows: (1) *N-cadherin* loss of function: *y w hsFLP UAS-CD8-GFP/+; Ncad^{M19} FRT^{40A} / tubP-Gal80 FRT^{40A} Gal4-GH146; y w hsFLP UAS-CD8-GFP/+; Ncad^{M19} Gal4-Mz19 FRT^{40A} / tubP-Gal80 FRT^{40A}*; (2) PN phenotype analysis in presence of *N-cadherin* mutant ORNs: *y w eyFLP/UAS-CD8-GFP; Gal4-Mz19 Ncad^{M19} FRT^{40A}/FRT^{40A} cl(2L)*; (3) ORN phenotype analysis in presence of *N-cadherin* mutant PNs: *y w hsFLP UAS-CD8-GFP/+; Ncad^{M19} FRT^{40A} / tubP-Gal80 FRT^{40A} Gal4-GH146; OR47b-CD2/+*; (4) *N-cadherin* reverse MARCM: *y w hsFLP UAS-CD8-GFP/+; tubP-Gal80 Ncad^{M19} FRT^{40A}/FRT^{40A} Gal4-GH146*; (5) *N-cadherin* rescue: *y w hsFLP UAS-CD8-GFP/UAS-Ncad(7a, 13a, 18a); Ncad^{M19} FRT^{40A} / tubP-Gal80 FRT^{40A} Gal4-GH146*; and (6) *N-cadherin* MARCM overexpression: *y w hsFLP UAS-CD8-GFP/ UAS-Ncad(7a, 13a, 18a); FRT^{40A} / tubP-Gal80 FRT^{40A} Gal4-GH146*.

Mutant alleles of other cadherin superfamily members tested are *fmi^{E59}* (Usui et al., 1999), *ft$^{l(2)fd}$* and *ds^{38}* (Yang et al., 2002), and *shg^{R69}*(Godt and Tepass, 1998).

Or47b-CD2 Construct and Transgenes

The rat CD2 coding region (Dunin-Borkowski and Brown, 1995) was cloned downstream of the *Drosophila* Or47b promoter element (Vosshall et al., 1999) in a pCasper vector to generate the Or47b-CD2 transgene (E. Marin, T. Chihara, and L.L., unpublished data).

Immunochemistry

The procedures for fixation, immunochemistry, and imaging were as described (Jefferis et al., 2001). Additional antibodies used in this study were rat monoclonal anti-N-cadherin antibody (Iwai et al., 1997), 1:30; rabbit anti-GFP serum (Molecular Probes), 1:500; and mouse monoclonal anti-CD2 antibody (OX34, Serotec), 1:100. Triple immunofluorescence with anti-CD2, nc82, and CD8 antibodies was carried out with Zenon Alexa Fluo 647 mouse IgG1 labeling kit (Molecular Probes).

3D Reconstruction

Confocal stacks of DL1 axons were imported into Neurolucida (Microbrightfield, Colchester, VT), and the GFP signals were manually reconstructed. The number of axon terminals and branches were counted with Neuroexplorer.

Acknowledgments

We are very grateful to E. Marin and T. Chihara for sharing the previously unpublished *47b-CD2* transgenic flies; D. Berdnik for sharing information about the *eyFLP* characterization; T. Uemura for N-cadherin mutants, transgenes, and antibodies; E. Buchner, T. Clandinin, M. Peifer, M. Simon, and L. Vosshall for antibodies, constructs, and fly strains; and S.L. Zipursky and T. Hummel for many fruitful discussions and communications of results prior to publication. We thank T. Clandinin, S. McConnell, T. Chihara, G. Jefferis, T. Komiyama, E. Marin, O. Schuldiner, and D. Berdnik for discussions and critical reading of this manuscript. This work was supported by a NIDCD grant (R01-DC005982) to L.L. H.Z. is a recipient of an individual Kirschstein-NRSA postdoctoral fellowship.

Received: December 9, 2003
Revised: February 9, 2004
Accepted: February 24, 2004
Published: April 7, 2004

References

Axel, R. (1995). The molecular logic of smell. Sci. Am. *273*, 154–159.

Buck, L.B. (2000). The molecular architecture of odor and pheromone sensing in mammals. Cell *100*, 611–618.

Devaud, J.M., Acebes, A., Ramaswami, M., and Ferrus, A. (2003). Structural and functional changes in the olfactory pathway of adult *Drosophila* take place at a critical age. J. Neurobiol. *56*, 13–23.

Dumstrei, K., Wang, F., Nassif, C., and Hartenstein, V. (2003). Early development of the *Drosophila* brain. V. Pattern of postembryonic neuronal lineages expressing DE-cadherin. J. Comp. Neurol. *455*, 451–462.

Dunin-Borkowski, O.M., and Brown, N.H. (1995). Mammalian CD2 is an effective heterologous marker of the cell surface in *Drosophila*. Dev. Biol. *168*, 689–693.

Godt, D., and Tepass, U. (1998). *Drosophila* oocyte localization is mediated by differential cadherin-based adhesion. Nature *395*, 387–391.

Hummel, T., and Zipursky, S.L. (2004). Afferent induction of olfactory glomeruli requires N-cadherin. Neuron *42*, this issue, 77–88.

Hummel, T., Vasconcelos, M.L., Clemens, J.C., Fishilevich, Y., Vosshall, L.B., and Zipursky, S.L. (2003). Axonal targeting of olfactory receptor neurons in *Drosophila* is controlled by Dscam. Neuron *37*, 221–231.

Hynes, R.O., and Zhao, Q. (2000). The evolution of cell adhesion. J. Cell Biol. *150*, F89–F96.

Ito, K., and Hotta, Y. (1992). Proliferation pattern of postembryonic neuroblasts in the brain of *Drosophila melanogaster*. Dev. Biol. *149*, 134–148.

Iwai, Y., Usui, T., Hirano, S., Steward, R., Takeichi, M., and Uemura, T. (1997). Axon patterning requires DN-cadherin, a novel neuronal adhesion receptor, in the *Drosophila* embryonic CNS. Neuron *19*, 77–89.

Jefferis, G.S.X.E., Marin, E.C., Stocker, R.F., and Luo, L. (2001). Target neuron prespecification in the olfactory map of *Drosophila*. Nature *414*, 204–208.

Jefferis, G.S.X.E., Marin, E.C., Watts, R.J., and Luo, L. (2002). Development of neuronal connectivity in *Drosophila* antennal lobes and mushroom bodies. Curr. Opin. Neurobiol. *12*, 80–86.

Jefferis, G.S.X.E., Vyas, R.M., Berdnik, D., Ramaekers, A., Stocker, R.F., Tanaka, N., Ito, K., and Luo, L. (2004). Developmental origin of wiring specificity in the olfactory system of *Drosophila*. Development *131*, 117–130.

Kaibuchi, K., Kuroda, S., Fukata, M., and Nakagawa, M. (1999).

Regulation of cadherin-mediated cell-cell adhesion by the Rho family GTPases. Curr. Opin. Cell Biol. *11*, 591–596.

Keller, A., and Vosshall, L.B. (2003). Decoding olfaction in *Drosophila*. Curr. Opin. Neurobiol. *13*, 103–110.

Komiyama, T., Johnson, W.A., Luo, L., and Jefferis, G.S. (2003). From lineage to wiring specificity: POU domain transcription factors control precise connections of *Drosophila* olfactory projection neurons. Cell *112*, 157–167.

Lee, T., and Luo, L. (1999). Mosaic analysis with a repressible cell marker for studies of gene function in neuronal morphogenesis. Neuron *22*, 451–461.

Lee, T., and Luo, L. (2001). Mosaic analysis with a repressible cell marker (MARCM) for *Drosophila* neural development. Trends Neurosci. *24*, 251–254.

Lee, T., Winter, C., Marticke, S.S., Lee, A., and Luo, L. (2000). Essential roles of *Drosophila* RhoA in the regulation of neuroblast proliferation and dendritic but not axonal morphogenesis. Neuron *25*, 307–316.

Lee, C.H., Herman, T., Clandinin, T.R., Lee, R., and Zipursky, S.L. (2001). N-cadherin regulates target specificity in the *Drosophila* visual system. Neuron *30*, 437–450.

Lin, D.M., Wang, F., Lowe, G., Gold, G.H., Axel, R., Ngai, J., and Brunet, L. (2000). Formation of precise connections in the olfactory bulb occurs in the absence of odorant-evoked neuronal activity. Neuron *26*, 69–80.

Malun, D., and Brunjes, P.C. (1996). Development of olfactory glomeruli: temporal and spatial interactions between olfactory receptor axons and mitral cells in opossums and rats. J. Comp. Neurol. *368*, 1–16.

Marin, E.C., Jefferis, G.S.X.E., Komiyama, T., Zhu, H., and Luo, L. (2002). Representation of the glomerular olfactory map in the *Drosophila* brain. Cell *109*, 243–255.

Newsome, T.P., Asling, B., and Dickson, B.J. (2000). Analysis of *Drosophila* photoreceptor axon guidance in eye-specific mosaics. Development *127*, 851–860.

Rhee, J., Mahfooz, N.S., Arregui, C., Lilien, J., Balsamo, J., and VanBerkum, M.F. (2002). Activation of the repulsive receptor Roundabout inhibits N-cadherin-mediated cell adhesion. Nat. Cell Biol. *4*, 798–805.

Shapiro, L., and Colman, D.R. (1999). The diversity of cadherins and implications for a synaptic adhesive code in the CNS. Neuron *23*, 427–430.

Stocker, R.F., Heimbeck, G., Gendre, N., and de Belle, J.S. (1997). Neuroblast ablation in *Drosophila* P[GAL4] lines reveals origins of olfactory interneurons. J. Neurobiol. *32*, 443–452.

Tepass, U., Gruszynski-DeFeo, E., Haag, T.A., Omatyar, L., Torok, T., and Hartenstein, V. (1996). shotgun encodes *Drosophila* E-cadherin and is preferentially required during cell rearrangement in the neurectoderm and other morphogenetically active epithelia. Genes Dev. *10*, 672–685.

Uemura, T., Oda, H., Kraut, R., Hayashi, S., Kotaoka, Y., and Takeichi, M. (1996). Zygotic *Drosophila* E-cadherin expression is required for processes of dynamic epithelial cell rearrangement in the *Drosophila* embryo. Genes Dev. *10*, 659–671.

Usui, T., Shima, Y., Shimada, Y., Hirano, S., Burgess, R.W., Schwarz, T.L., Takeichi, M., and Uemura, T. (1999). Flamingo, a seven-pass transmembrane cadherin, regulates planar cell polarity under the control of Frizzled. Cell *98*, 585–595.

Vosshall, L.B., Amrein, H., Morozov, P.S., Rzhetsky, A., and Axel, R. (1999). A spatial map of olfactory receptor expression in the *Drosophila* antenna. Cell *96*, 725–736.

Vosshall, L.B., Wong, A.M., and Axel, R. (2000). An olfactory sensory map in the fly brain. Cell *102*, 147–159.

Wong, A.M., Wang, J.W., and Axel, R. (2002). Spatial representation of the glomerular map in the *Drosophila* protocerebrum. Cell *109*, 229–241.

Wu, Q., and Maniatis, T. (1999). A striking organization of a large family of human neural cadherin-like cell adhesion genes. Cell *97*, 779–790.

Yagi, T., and Takeichi, M. (2000). Cadherin superfamily genes: functions, genomic organization, and neurologic diversity. Genes Dev. *14*, 1169–1180.

Yang, C.H., Axelrod, J.D., and Simon, M.A. (2002). Regulation of Frizzled by fat-like cadherins during planar polarity signaling in the *Drosophila* compound eye. Cell *108*, 675–688.

Yap, A.S., Brieher, W.M., and Gumbiner, B.M. (1997). Molecular and functional analysis of cadherin-based adherens junctions. Annu. Rev. Cell Dev. Biol. *13*, 119–146.

Yasuyama, K., Meinertzhagen, I.A., and Schurmann, F.W. (2002). Synaptic organization of the mushroom body calyx in *Drosophila melanogaster*. J. Comp. Neurol. *445*, 211–226.